# 11 PULSATIONS AND MAGNETOHYDRODYNAMIC WAVES

M. G. Kivelson

### 11.1 INTRODUCTION

WHEN PHYSICAL SYSTEMS experience perturbations, it is common for them to respond by emitting waves. For example, a sound wave in a gas like the atmosphere is produced by a change in pressure at the source of the wave, whether it is a hi-fi speaker system or a dynamite blast. The pressure perturbation then travels through the atmosphere. By knowing the properties of the atmosphere, one can predict the speed at which the signal will propagate, the local speed of sound:  $c_s = (\gamma p/\rho)^{\frac{1}{2}}$ , where  $\gamma$  is the ratio of the specific heat at constant pressure to the specific heat at constant volume in the gas, p is the gas pressure, and  $\rho$ is the gas density. An electromagnetic wave in a vacuum or in a dielectric medium can be established by driving a time-varying current in an antenna. Here, too, it is possible to predict the speed at which the signal will propagate, provided that one can characterize the medium. Conversely, various properties of a system can be probed by measuring the properties of waves found within it, such as frequency, wavelength, and polarization. For example, in the relation  $f\lambda = \text{constant}$ , between the frequency f and the wavelength  $\lambda$  of an electromagnetic wave in an isotropic medium, the value of the constant provides information on the dielectric properties of the system. The wave polarization (for an electromagnetic wave specified by the direction of the varying electric field of the wave) is related to the wave's propagation direction. For an electromagnetic wave in a vacuum, the plane of the electric and magnetic perturbations is always normal to the direction of propagation. Sound waves, on the other hand, are polarized along the direction of propagation, the polarization direction being that of the gradient of fluctuating pressure. For a closed system, the oscillations normally are combinations of standing waves whose frequencies are governed by the size of the system, as well as by its material properties.

In a plasma, as in a gas, we might expect to find waves that are similar to sound waves, but a plasma is composed principally of charged particles that carry currents. Thus, its electromagnetic properties are of paramount importance, but plasma density and pressure are also relevant. As a consequence, plasma waves differ from both sound waves and electromagnetic waves.

 TABLE 11.1.
 Ranges of Periods and Frequencies in Different Pulsation Classes

	Pc-1	Pc-2	Pc-3	Pc-4	Pc-5	Pi-1	Pi-2
T (s)	0.2-5	5–10	10-45	45–150	150-600	1–40	40-150
	0.2-5 Hz	0.1–0.2 Hz	22-100 mHz	7–22 mHz	2-7 mHz	0.025–1 Hz	2-25 mHz

In this chapter, we discuss the nature of the lowest-frequency waves that occur in plasmas. A "low" frequency must be lower than the natural frequencies of the plasma, such as the plasma frequency  $f_p$  and the ion gyrofrequency  $f_{ci}$  that were introduced in Chapter 2. Such waves are referred to as ultra-low-frequency waves. Higher-frequency waves will be treated in Chapter 12. We shall show that the combination of mechanical forces (present because of the gaslike properties of the plasma) and electromagnetic forces (present because the particles are charged) creates unique types of waves: magnetohydrodynamic (MHD) waves. We shall point out how they differ from the waves found in neutral dielectric media.

The equations for conducting fluids, basically expressions of Newton's laws of motion and Maxwell's equations (Maxwell, 1873), were known to physicists for more than half a century before it was recognized that electromagnetic waves can propagate in conducting fluids even though they cannot propagate in rigid conductors. The MHD wave solutions were eventually derived by Hannes Alfvén (1942), but direct confirmation of the existence of the waves was difficult to obtain, as they decay rapidly in most laboratory situations. One can show that the decay rate can be small only if the spatial scale of the system is sufficiently large. Thus it was that the study of Alfvén's predicted waves became principally the task of space physicists.

The first observations of ultra-low-frequency (ULF) fluctuations (with periods ranging from seconds to minutes) of magnetic fields were made on the ground (Stewart, 1861), almost a century before their links to plasmas in near-earth space were established. Early studies of the magnetic pulsations measured by ground-based observers noted that waves could be grouped into classes that appeared to differ in fundamental ways. Some were continuous pulsations, quasi-sinusoidal in form, and each with a well-defined spectral peak. These were called Pc pulsations, and they were broken into subgroups on the basis of their periods (starting with Pc-1 in the 0.2-5-Hz band and ending with Pc-5 in the 1.7-6.7-mHz band). Other pulsations in the same frequency band contained power at many different frequencies. Such waves were called Pi for irregular pulsations. The names assigned to different frequency bands (Jacobs et al., 1964) are shown in Table 11.1. Typical magnetic-pulsation signatures are illustrated in Figure 11.1, which includes both groundbased observations from a chain of stations at different latitudes and

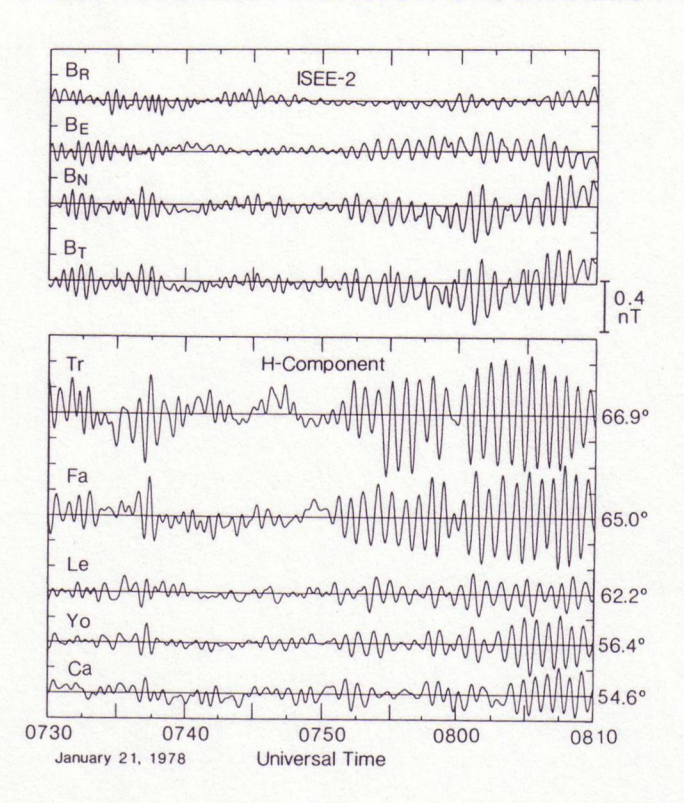


FIG. 11.1 Examples of approximately 1-min waves in the magnetosphere (upper panels) and on the ground (lower panels) at stations whose latitudes are indicated to the right.

simultaneous measurements from a spacecraft in the near-equatorial magnetosphere.

Dungey (1954a,b) was the first to suggest that MHD waves in the outer atmosphere were the sources of the oscillating or pulsating magnetic fields observed on the surface. In particular, the distinct periods of Pc pulsations suggested a resonant process, and Dungey proposed that the pulsations were caused by waves standing along magnetic-field lines and reflected at the ionospheres at the two ends. That idea has been further developed and is generally supported by studies of both ground-based and spacecraft data. We shall return to it after developing the theory and deriving some of the properties of MHD waves in a conducting fluid.

### 11.2 BASIC EQUATIONS

MHD waves are found as solutions to the equations introduced in Chapter 2 to express the conservation laws and Maxwell's equations. They are repeated here for convenience. Equation (2.29b) guarantees that mass is conserved as the fluid moves:

$$\frac{\partial \rho}{\partial t} + \nabla \cdot \rho \mathbf{u} = 0 \qquad \text{(continuity equation)} \tag{11.1}$$

Momentum conservation is assured by equation (2.32), in which we set  $\mathbf{F}_{o} = 0$  and assume neither sources nor losses:

$$\rho \left( \frac{\partial \mathbf{u}}{\partial t} + \mathbf{u} \cdot \nabla \mathbf{u} \right) = -\nabla p + \mathbf{j} \times \mathbf{B}$$
(11.2)

Maxwell's equations in the low-frequency limit [equations (2.35), (2.36b), and (2.37)] will be needed. These equations are

$$\frac{\partial \mathbf{B}}{\partial t} = -\nabla \times \mathbf{E} \qquad \text{(Faraday's law)} \tag{11.3}$$

$$\nabla \times \mathbf{B} = \mu_0 \mathbf{j}$$
 (Ampère's law) (11.4)

and the requirement that **B** be divergenceless:

$$\nabla \cdot \mathbf{B} = 0 \tag{11.5}$$

We add Ohm's law in the form [equation (2.46)]

$$\mathbf{E} + \mathbf{u} \times \mathbf{B} = 0 \tag{11.6}$$

and an equation that states that the specific entropy (entropy per unit volume) is conserved in the convecting magnetized plasma:

$$\left(\frac{\partial}{\partial t} + \mathbf{u} \cdot \nabla\right) \left(\frac{p}{\rho^{\gamma}}\right) = 0 \tag{11.7}$$

Here, as in earlier chapters, p is the pressure,  $\rho$  is the mass density, u is the flow velocity, j is the electric-current density, B is the magnetic field (magnetic induction),  $\mu_0$  is the magnetic permeability of free space, E is the electric field, and  $\gamma$  is the ratio of the specific heat at constant pressure to the specific heat at constant volume;  $\gamma$  is frequently referred to as the polytropic index.

As the derivative acting on the expression in parentheses on the right in (11.7) is just the time rate of change in a frame that follows the plasma as it flows through the system, the equation requires that the plasma obey an adiabatic equation of state. In most space plasmas,  $\gamma$  is  $\frac{5}{3}$ .

We can express the current in terms of the magnetic field, and the electric field in terms of u and B, by using (11.4) and (11.6). Equation (11.2) becomes

$$\rho \left( \frac{\partial \mathbf{u}}{\partial t} + \mathbf{u} \cdot \nabla \mathbf{u} \right) = -\nabla p + (\nabla \times \mathbf{B}) \times \mathbf{B} / \mu_0$$
(11.8)

Suppose that the variations in a system are only in the x-direction and that  $\mathbf{B} = B\hat{\mathbf{z}}$ . Then the right-hand side of (11.8) can be written as

$$-\hat{\mathbf{x}} \left( \frac{\partial p}{\partial x} + \frac{B}{\mu_0} \frac{\partial B}{\partial x} \right)$$

and the x-component of the momentum equation takes the form

$$\rho \left( \frac{\partial u_x}{\partial t} + u_x \frac{\partial u_x}{\partial x} \right) = -\frac{\partial}{\partial x} [p + (B^2/2\mu_0)]$$
(11.9)

As discussed in relation to equation (2.48), the quantity  $B^2/2\mu_0$  is the magnetic pressure. The fluid momentum responds to gradients of both the magnetic and thermal pressures.

The set of equations (11.1)–(11.7) or the modified forms that follow must be simultaneously satisfied. Plasma structures that remain at rest in the moving fluid compose a particularly simple subset of solutions of this collection of equations. Such spatially varying plasma properties appear as time variations to an observer not moving with the flow. Using the density  $\rho$  as an example, one finds that if  $\rho = \rho(\mathbf{x})$  in the plasma rest frame, it depends on space and time in the form

$$\rho(\mathbf{x}, t) = \rho \left( \mathbf{x} - \int_{t_0}^t dt' \ \mathbf{u}(\mathbf{x}, t') \right)$$
 (11.10)

in the observer's frame. Here,  $t_0$  is the time when the fluid element is at  $\mathbf{x} = \mathbf{0}$ . This form automatically satisfies equations (11.1) and (11.7), as the sum of the two derivatives vanishes independently of the form of  $\rho(\mathbf{x})$  in the plasma rest frame. The additional equations are satisfied if  $\mathbf{u}$ , p, and  $\mathbf{B}$  are constant. This solution is referred to as an entropy "wave." The reference to entropy reflects the fact that if  $\rho$  varies at constant pressure, then the specific entropy  $p/\rho^{\gamma}$  varies.

There is another nonpropagating solution with **k** perpendicular to **B** for which the total pressure  $p + B^2/2\mu_0$  is constant across planar surfaces that convect with the flow. In order to satisfy all of the required equations, the component of **B** normal to the surface must vanish, and the normal component of **u** must not change across the surface. The components of both **B** and **u** tangential to the surface may vary. This solution is the limit of the slow mode for  $\mathbf{k} \perp \mathbf{B}$ . In the nonlinear regime, the entropy wave relates to the contact discontinuity, and the slow-mode wave relates to the tangential discontinuity.

### 11.3 EQUATIONS FOR LINEAR WAVES

The preceding section described a convecting perturbation of arbitrary amplitude that satisfies the set of equations. This section describes a set of waves that propagate relative to the fluid. For simplicity, we assume that the perturbations carried by the waves are small.

Let us assume that the plasma is initially at rest, which means that there are neither flows nor electric fields, and also assume that no currents are flowing. The wave perturbations introduce finite but small **E**, **u**, and **j**. The magnetic field, mass density, and pressure also change, so that

$$\mathbf{B} \to \mathbf{B} + \mathbf{b}, \qquad \rho \to \rho + \delta \rho, \qquad p \to p + \delta p$$

All of the perturbed quantities, **b**,  $\delta \rho$ ,  $\delta p$ , **u**,  $\mathbf{E} = -\mathbf{u} \times \mathbf{B}$ , and  $\mathbf{j} = \nabla \times \mathbf{b} / \mu_0$ , are assumed to be small enough that only terms linear in any of them need be retained. This means that squares or high powers and cross products will be dropped. The perturbed quantities then must satisfy the equations

$$\frac{\partial \delta \rho}{\partial t} + \rho \nabla \cdot \mathbf{u} = 0 \tag{11.1'}$$

$$\rho \frac{\partial \mathbf{u}}{\partial t} = -\nabla \delta p + (\nabla \times \mathbf{b}) \times \mathbf{B}/\mu_0 \tag{11.8'}$$

$$\frac{\partial \mathbf{b}}{\partial t} = \nabla \times (\mathbf{u} \times \mathbf{B}) \tag{11.3'}$$

We must have  $\nabla \cdot \mathbf{b} = 0$  to satisfy equation (11.5). If this condition holds initially, the divergence of (11.3')  $[(\partial/\partial t)(\nabla \cdot \mathbf{b} = 0)]$  shows that the condition is automatically satisfied at all times.

The adiabatic requirement also becomes an initial condition, because

$$\frac{\partial \delta p}{\partial t} = \frac{\gamma p}{\rho} \frac{\partial \delta \rho}{\partial t} = c_s^2 \frac{\partial \delta \rho}{\partial t}$$

becomes

$$\frac{\partial}{\partial t} \left( \frac{\delta p}{c_s^2 \delta \rho} \right) = 0$$

and the constant value of the ratio of  $\delta p$  to  $\delta \rho$  is set by the initial conditions. Substitution of  $\delta p$  in terms of  $\delta \rho$  leaves us with seven unknowns that describe the wave perturbations:  $\delta \rho$ , **u**, and **b**, and seven equations: (11.1'), (11.8'), and (11.3'), once again counting each component of a vector equation separately. In the following sections, we shall solve for the wave properties, making various simplifying assumptions.

### 11.4 WAVES IN COLD PLASMAS

The simplest system in which MHD waves exist is a cold magnetized plasma. The concept of "cold" needs to be defined, because the temperature need not be zero. All that is meant is that the plasma pressure [which is given by equation (2.33)] is unimportant. Equation (11.9) shows that if the ratio of the plasma pressure to the magnetic pressure is small [i.e.,  $\beta \le 1$ , where  $\beta$  is defined in equation (2.49)], then the plasma pressure is not important.

In describing the properties of waves, it is convenient to introduce the exponential notation

$$e^{ix} = \cos x + i \sin x \tag{11.11}$$

Expressing the solution of a differential equation in complex exponential form simplifies the derivation, because the derivative of an exponential is just a multiple of the original exponential. However, any equation written in terms of the complex exponential must be satisfied separately by the terms proportional to i and the terms independent of i, and this requirement is equivalent to solving the equation in terms of sines and cosines.

For a plane wave propagating in the x-direction, with wavelength  $\lambda$  and frequency f, the oscillating quantities can be taken as proportional to

$$e^{ikx}e^{-i\omega t} = e^{i(kx - \omega t)} \tag{11.12}$$

where  $k=2\pi/\lambda$  and  $\omega=2\pi f$ . If the proportionality factors are complex, the different perturbed quantities may have arbitrary relative phase,  $\delta$ , where tan  $\delta$  is the ratio of the imaginary part to the real part of the amplitude factor. The solution is, in any case, oscillatory. At a fixed spatial location, the solution oscillates in time with frequency f, and at a fixed time, the solution oscillates spatially with a wavelength  $\lambda$ . Notice that in the second form of (11.12) the argument of the exponential is constant if  $x=x_0+(\omega/k)t$ . This means that the solutions are constant at a position that moves along the x-axis with a velocity  $dx/dt=\omega/k$ , that is, at the wave phase velocity [equation (2.50a)]:

$$v_{\rm ph} = \omega/k \tag{11.13}$$

We use equations (11.1'), (11.8'), and (11.3'), writing them in the forms that apply to the cold-plasma limit (p=0). In doing so, we shall also assume that the background magnetic field and the plasma density are constant (i.e.,  $\partial \rho/\partial x = 0$ ,  $\partial \mathbf{B}/\partial x = 0$ ,  $\partial \rho/\partial t = 0$ , and  $\partial \mathbf{B}/\partial t = 0$ ) and that the wave is moving along the x-direction, meaning that only the derivatives in x and t need be retained:

$$\frac{\partial \delta \rho}{\partial t} + \rho \, \frac{\partial u_x}{\partial x} = 0 \tag{11.14}$$

$$\rho \frac{\partial \mathbf{u}}{\partial t} = -\hat{\mathbf{x}} \frac{\partial (\mathbf{b} \cdot \mathbf{B}/\mu_0)}{\partial x} + \left(\frac{B_x}{\mu_0}\right) \frac{\partial \mathbf{b}}{\partial x}$$
(11.15)

$$\frac{\partial \mathbf{b}}{\partial t} = B_x \frac{\partial \mathbf{u}}{\partial x} - \left(\frac{\partial u_x}{\partial x} \mathbf{B}\right) \tag{11.16}$$

The assumed exponential dependence on x and t of the wave properties  $(\delta \rho, \mathbf{u}, \text{ and } \mathbf{b})$  implies that time and x derivatives can be replaced by  $-i\omega$  and -ik, respectively. Then these equations become

$$i(\omega\delta\rho - k\rho u_x) = 0 \tag{11.14'}$$

$$i[\omega \rho \mathbf{u} - k(\hat{\mathbf{x}}(\mathbf{b} \cdot \mathbf{B}) - B_x \mathbf{b})/\mu_0] = 0$$
(11.15')

$$i[\boldsymbol{\omega}\mathbf{b} + k(\boldsymbol{B}_{x}\mathbf{u} - \boldsymbol{u}_{x}\mathbf{B})] = 0 \tag{11.16'}$$

The equations are now just a set of algebraic equations, which are easy to deal with. One need only eliminate variables by substitution. Without

loss of generality, we can assume that **B** lies in the x-z plane, and we have already assumed that  $\mathbf{k} = k\hat{\mathbf{x}}$ , and so  $\mathbf{B} = (B\cos\theta, 0, B\sin\theta)$ . Here  $\theta$  is the angle between **B** and  $\mathbf{k}$ . By elimination, we can obtain

$$[(\omega/k)^2 - v_A^2 \sin^2 \theta] u_x + v_A^2 \sin \theta \cos \theta u_z = 0$$
 (11.17a)

$$[(\omega/k)^2 - v_A^2 \cos^2 \theta] u_v = 0$$
 (11.17b)

$$[(\omega/k)^2 - v_A^2 \cos^2 \theta] u_z + v_A^2 \sin \theta \cos \theta u_x = 0$$
 (11.17c)

$$v_{\rm A} = (B^2/\mu_0 \rho)^{\frac{1}{2}}$$

The coefficients in (11.17) are squares of velocities, with  $\omega/k$  the wave phase velocity and  $v_A$  the Alfvén velocity [see equation (2.51)]. Equations (11.17a-c) are homogeneous equations that have solutions only if the determinant of their coefficients vanishes. This requirement gives an equation for  $v_{\rm ph} = \omega/k$  that is called a dispersion relation. The roots of the dispersion relation give the values of the phase velocity for MHD waves in the cold plasma:

$$(\omega/k)^2 = v_A^2 \cos^2 \theta \tag{11.18a}$$

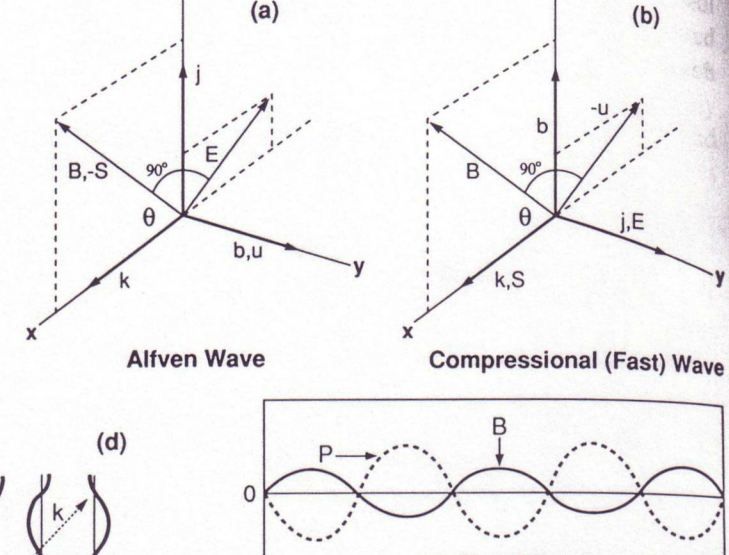
$$(\omega/k)^2 = v_A^2 \tag{11.18b}$$

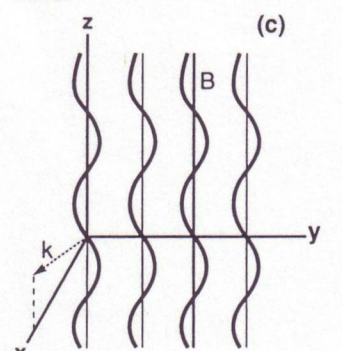
Dispersion relations such as (11.18a) and (11.18b) impose relations between the frequency and the vector wave number that must be satisfied in order for a wave to exist in the plasma. The requirements that electromagnetic waves in free space propagate at the speed of light ( $\omega/k = c$ , or the equivalent form in terms of frequency and wavelength) or that sound waves in a neutral gas propagate at the speed of sound ( $\omega/k = c_s$ ) are familiar examples of dispersion relations. Equations (11.18a) and (11.18b) show that the dispersion relations of waves in magnetized plasmas depend on the magnitude of the magnetic field, the density of the plasma, and, under some conditions, the direction of wave propagation. Except for  $\theta = 0$ , the two equations cannot both be satisfied for the same k and  $\omega$ , and so the dispersion relation implies two independent solutions.

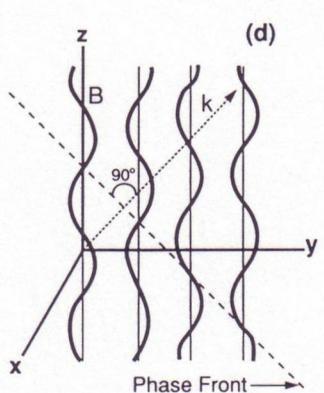
It is important to remember that a solution is valid only if all three of the equations (11.17a-c) are satisfied. Consider first the wave that satisfies the dispersion relation (11.18a), referred to as the *shear Alfvén wave*. By substituting (11.18a) into (11.17a-c), we see that (11.17b) is satisfied for any value of  $u_y$ , but (11.17a) and (11.17c) are satisfied only if  $u_x = u_z = 0$ . Thus the shear Alfvén wave propagates with the phase velocity  $v_A \cos \theta$  and sets the fluid into motion in the direction perpendicular to the plane containing the propagation vector  $\mathbf{k}$  and the background field. Other parameters of the wave, such as its electric and magnetic perturbations, can be expressed in terms of  $u_y$  by using (11.6), (11.16'), and so forth, and setting  $u_x = 0$  and  $u_z = 0$ . Equation (11.14') shows that this type of wave does not change the density of the fluid (because  $u_x = 0$ ). The relative orientations of the perturbation vectors in this type of wave are illustrated in Figure 11.2a. Because the perturbation of the

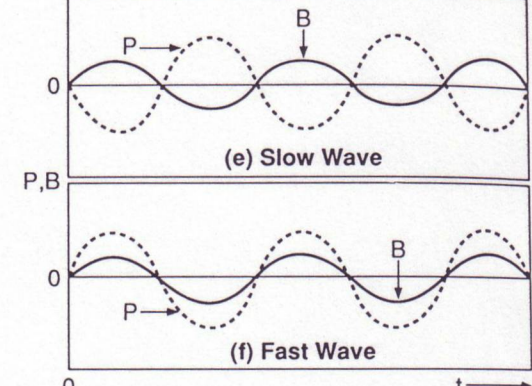
338

FIG.11.2. Schematic of wave polarizations for (a) the Alfvén wave and (b) the fast compressional wave. Displacements of the field lines (thick curves) at maximum displacement for (c) the Alfvén wave and (d) the fast compressional wave. The thin lines represent the unperturbed field. Plasma-pressure and magnetic-pressure perturbations versus time for (e) the slow compressional wave and (f) the fast compressional wave.









magnetic field is perpendicular to the background field, the field magnitude is constant (to linear order in the perturbation field) even in the presence of the wave:

$$|\mathbf{B} + \mathbf{b}|^2 \approx B^2 + 2\mathbf{B} \cdot \mathbf{b} = B^2$$

As the foregoing identity implies that the magnetic pressure (which is the only relevant pressure in a cold plasma) is constant, the wave is noncompressional.

The second dispersion relation (11.18b) automatically satisfies (11.17a) and (11.17c) for any value of  $u_x$  and  $u_z$ , but the only way to satisfy (11.17b) is to set  $u_y = 0$ . This means that a second type of wave can exist, one that sets the fluid into motion within the plane containing **k** and **B**. As  $u_x$  does not vanish, (11.14') implies that this type of wave changes the fluid density. As well, nonvanishing perturbations of the field magnitude are produced. This can be seen as follows:

$$|\mathbf{B} + \mathbf{b}|^2 \approx B^2 + 2\mathbf{B} \cdot \mathbf{b} = B^2 + 2ku_x B^2/\omega$$

where (11.15') and (11.16') have been used to obtain the final form. As  $u_x$  does not vanish, the magnitude of the field and the magnetic pressure will fluctuate when the wave is present. That is why this type of wave is

often referred to as a *compressional wave*. Figure 11.2b shows the polarization of the wave schematically. The wave energy propagates along the direction of the Poynting flux vector:

$$\mathbf{S} = \frac{1}{\mu_0} \mathbf{E} \times \mathbf{b}$$

This direction is along  $\pm \mathbf{B}$  in the shear Alfvén wave, but at an arbitrary angle (parallel to k) relative to  $\mathbf{B}$  in the compressional wave. This is an important aspect that distinguishes the two wave modes. Figures 11.2c and 11.2d show schematics of the displaced field lines in shear Alfvén waves and fast waves, respectively. In the shear Alfvén waves, the perturbations are all perpendicular to  $\mathbf{B}$ , and the distance between the perturbed field lines is constant. In the fast wave, the perturbations are oblique to  $\mathbf{B}$ , and the oblique phase fronts result in varying separations between the perturbed field lines.

If the wave propagates in directions other than along the background magnetic field (i.e., if  $\theta \neq 0$ ), the phase velocity (11.18b) is larger than (11.18a). For this reason, the compressional mode is also referred to as the *fast mode*.

An additional property of interest in a wave analysis is what is referred to as the *group velocity*,  $\mathbf{v}_g$ . It describes the velocity of energy or information transfer by a physically realistic wave packet that is not strictly monochromatic and may contain a spread of wave vectors. Such a wave packet can be described as a superposition of monochromatic waves using Fourier analysis. Examples have been worked out by Jackson (1962) for the case of electromagnetic waves in dielectric media, but the approach applies to plasma waves as well. The analysis shows that if the spreads about the mean are sufficiently small, an expansion

$$\omega = \omega_0 + (\mathbf{k} - \mathbf{k}_0) \cdot \nabla_k \omega$$

can be introduced. The pulse then retains its shape and propagates with the (vector) velocity  $\mathbf{v}_g = \nabla_k \omega$  [see equation (2.50b)]. Note that this is a vector velocity, which is found by expressing  $\omega$  as a function of the vector  $\mathbf{k}$  and taking derivatives with respect to its components. For the two types of waves we have discussed, we find

$$\mathbf{v}_g = v_A \hat{\mathbf{B}}$$
 (for the shear Alfvén wave) (11.19a)

$$\mathbf{v}_g = v_A \hat{\mathbf{k}}$$
 (for the fast-mode wave) (11.19b)

where  $\hat{\mathbf{B}}$  and  $\hat{\mathbf{k}}$  are unit vectors along  $\mathbf{B}$  and  $\mathbf{k}$ . These equations tell us that the fast-mode wave can carry energy and information in any direction, whereas the energy and information content of a shear Alfvén wave are strictly guided along the background field, even if phase fronts are oriented arbitrarily.

### 11.5 WAVES IN WARM PLASMAS

In a warm plasma, the plasma-pressure terms cannot be dropped from the equations (i.e.,  $\beta$  is no longer small compared with unity). The pressure-gradient term must be considered in the momentum equation, and (11.7) is also needed. For small-amplitude perturbations, the linear-analysis approach is once again appropriate. We end up with a set of equations analogous to (11.17), and the requirement that the determinant of the coefficients vanish gives a dispersion relation

$$(\omega^2 - \cos^2\theta \ k^2 v_A^2)[\omega^4 - \omega^2 k^2 (c_s^2 + v_A^2) + \cos^2\theta \ k^4 v_A^2 c_s^2] = 0$$
 (11.20)

which has three solutions:

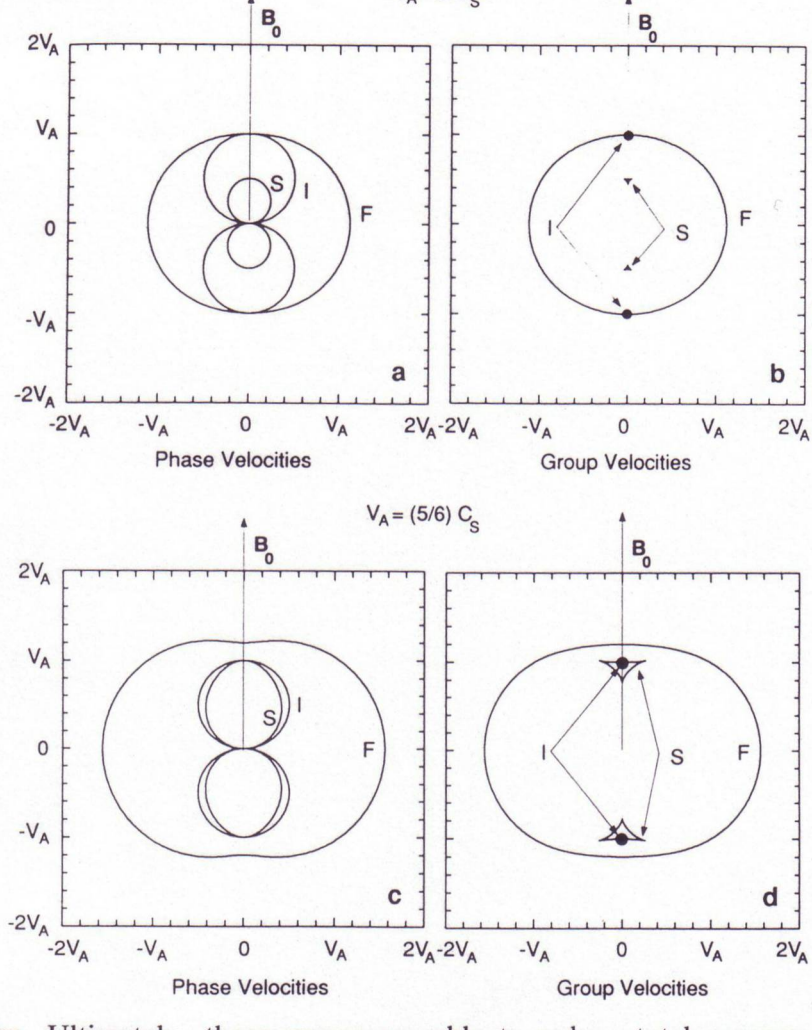
$$\omega^2 = v_A^2 \cos^2 \theta \ k^2 \tag{11.20a}$$

$$\omega^2/k^2 = \frac{1}{2} \{ c_s^2 + v_A^2 \pm \left[ (c_s^2 + v_A^2)^2 - 4c_s^2 v_A^2 \cos^2 \theta \right]^{\frac{1}{2}} \}$$
 (11.20b)

Comparing the dispersion relations (11.18) and (11.20), we find that the finite temperature of the plasma has introduced an additional wave mode and changed the properties of the fast mode previously discussed. The shear Alfvén mode appears again as the solution of (11.20a). Its phase velocity still depends only on the Alfvén velocity. All of its properties (e.g., polarization perpendicular to both B and k, and no change of density or field magnitude) remain the same as in the cold-plasma case.

The roots of (11.20b) depend not only on the Alfvén velocity but also on the sound speed. These roots apply to compressional wave modes (i.e., waves that do change the density and the field magnitude). The two solutions are referred to as the fast (positive sign) and the slow (negative sign) waves and are also called magnetoacoustic wave modes. The electric, magnetic, and current polarizations of the fast and slow waves are shown in Figure 11.2. However, when the thermal pressure varies along **B**, the flow velocity can have a parallel component, and **u** will not be perpendicular to **B**. The thermal-pressure perturbations that are a feature of waves in a warm plasma are in phase with the magnetic-pressure perturbations in the fast wave, but are out of phase with them in the slow wave. Figures 11.2e and 11.2f show schematically the phase relations of the field and pressure perturbations in fast and slow waves.

The fast mode is produced when the total pressure of the plasma (the sum of particle pressure and field pressure) changes locally in the system. For example, if the solar-wind pressure on the dayside of the magnetosphere increases suddenly, a gradient of total pressure, positive toward the dayside boundary, will develop. The pressure perturbation serves as a source of compressional waves [see equation (11.8'), where the pressure-gradient term is a source of plasma motion]. The waves have p and  $p_B$  in phase and are therefore fast-mode waves. As they radiate away from the boundary source, they carry away the excess



 $V_A = 2 C_S$ 

**FIG. 11.3.** Friedrichs diagrams for (a) the phase velocity and (b) the group velocity for  $v_A = 2c_s$  and (c) the phase velocity and (d) the group velocity for  $v_A = \frac{5}{6}c_s$ . Wave modes are fast (F), intermediate (I), and slow (S).

pressure. Ultimately, these waves are able to reduce total pressure gradients. This wave mode propagates almost isotropically.

A convenient way in which to represent the phase velocity of a wave is in a polar plot, referred to as a Friedrichs diagram, with one axis aligned with the background field. The angle relative to that axis is the angle between **k** and **B**, and the distance from the origin represents that phase velocity. This type of plot is given for the case  $c_s^2 < v_A^2$  in Figure 11.3a. For the fast wave, both the phase velocity and the group velocity are largest for propagation perpendicular to **B**. For the slow wave and the intermediate wave, the phase velocity vanishes for  $\mathbf{k} \perp \mathbf{B}$ .

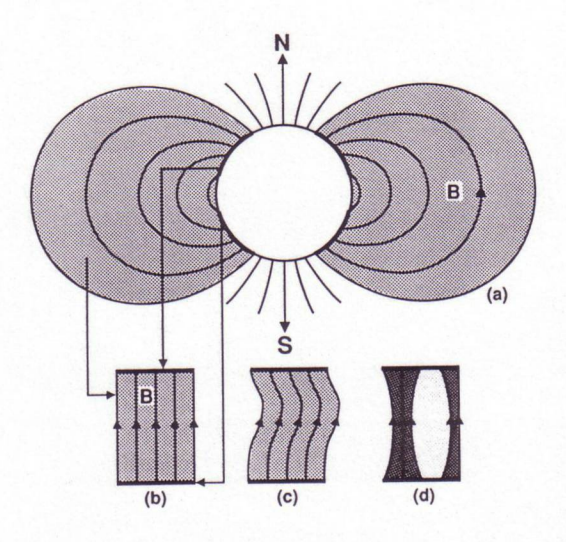
The group velocity can also be represented in a polar plot, this time with the angle relative to the **B**-direction representing the angle between **B** and the group velocity; the length of the vector represents the magnitude of the group velocity. The plot is shown in Figure 11.3b for the case  $c_s^2 < v_A^2$ . The fast-mode group velocity is finite in all directions and largest perpendicular to **B**. As pointed out in the discussion of Poynting

flux, these waves can carry energy in any direction, as  $\mathbf{v_g}$  remains finite at all angles. The intermediate wave has a group velocity that is along  $\pm \mathbf{B}$ , with amplitude  $v_A$  for all  $\mathbf{k}$ , and so it appears as a pair of points on the plot. This is consistent with the directions of  $\mathbf{S}$  in Figure 11.2. The slow-mode group velocity is  $\pm c_s$  for  $\mathbf{k}$  along  $\mathbf{B}$ . As the angle between  $\mathbf{k}$  and  $\mathbf{B}$  increases, the group velocity increases slightly and rotates a bit away from  $\mathbf{B}$ . As the angle continues to increase, the group velocity decreases and aligns more closely with  $\mathbf{B}$ . This accounts for the peculiar quasi-triangular curves in Figure 11.3b. Independent of  $\mathbf{k}$ , the slow-mode group velocity remains nearly aligned with  $\mathbf{B}$ . It carries energy only over a relatively narrow range of angles and is referred to as "field-guided."

The slow-mode wave is different from the fast-mode wave in several ways. For the slow mode, total pressure (i.e., the sum of particle pressure and magnetic pressure) is approximately constant across the background field. As described earlier, slow waves carry energy predominantly along the background field. Field-aligned gradients of the total pressure drive slow-mode waves. In particular, when the sound speed is much smaller than the Alfvén speed, the slow mode propagates along B at the sound speed and reduces plasma-pressure gradients. Figures 11.3c and 11.3d show the phase and group velocities, respectively, for the case  $c_s^2 > v_A^2$ . Qualitatively, the features of wave propagation are unchanged relative to the previous case, but for field-aligned propagation, the slow and intermediate modes adopt the Alfvén speed.

If fast- and slow-mode waves reduce pressure gradients, what does the shear Alfvén wave do? It acts to reduce the bending of the magnetic field. Plasma flow across the field can increase the bending of the field. The associated field perturbations will create currents that act to reduce the additional curvature of the field line. The closure of the currents that flow through the plasma is, in part, along the magnetic field, so that the shear Alfvén wave introduces field-aligned currents. Figure 11.2 shows that the perturbation current in the Alfvén wave (but not in the two compressional waves) has a nonvanishing component along **B**.

This discussion of MHD waves in warm plasmas links closely with the earlier discussion of shocks in Chapter 5. The shock develops when the information required to slow and divert a flow cannot propagate upstream fast enough. The pileup of waves unable to propagate upstream leads to nonlinear conditions that establish shocks in the flow. The shock front found farthest upstream of an obstacle is linked to the fast magnetoacoustic wave, the wave that propagates fastest, and in all directions, and serves to reduce pressure gradients and to slow and divert the flow. The intermediate wave propagates more slowly and nonisotropically. It serves to rotate the field. Only under special conditions can it develop into a shock. Most rotations observed in space plasmas appear to be unrelated to shocks. Slow-mode waves, because of their nonisotropic propagation, can play at most a limited role in



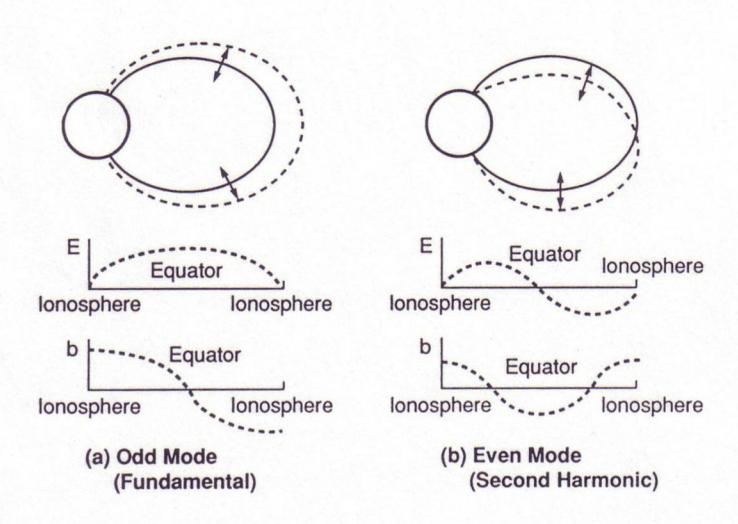
reducing pressure gradients, but slow shocks have been observed in space plasmas.

11.6 IONOSPHERIC BOUNDARY CONDITIONS

The frequencies of ULF waves that can be excited in a plasma depend not only on the wave modes but also on the boundary conditions. For the magnetosphere, the boundaries are the magnetopause and the ionosphere. Here we consider the conditions that must be satisfied at the ionospheric boundary of a flux tube. The ionosphere both reflects and transmits to the ground the ULF signals incident from above. We treat the ionosphere in a qualitative manner by representing it as a thin conducting sheet. The ionosphere lies above a neutral atmosphere that is in turn bounded by the earth. Figure 11.4 shows schematically a dipolar magnetosphere containing plasma (shown by stippling). In this figure, the high-latitude ionosphere forms boundaries at the ends of (most) field lines. The near-equatorial ionosphere serves as an inner boundary, and the magnetopause as an outer boundary. In Figure 11.4b, the field lines have been straightened to form a "box model" of the magnetosphere. If the conductivity of the ionosphere is very high, both the electric field and the wave displacement must vanish at the ionospheric ends of the field lines (as well as on the left side of the box). This means that any wave incident on the ionosphere will be reflected back toward the other ionosphere. (At lower conductivities, the waves are only partially reflected.) Like waves on a string, the Alfvén waves can satisfy the reflection condition only for certain selected wavelengths. If the length of the field line between the two ionospheres is l, the allowed wavelengths along the field direction  $\lambda_{\parallel}$  are

FIG. 11.4. Schematic (a, b) of the dipole field and its relation to a box model of the magnetosphere. Dipole field lines are straightened and bounded by the off-equatorial ionosphere at the top and bottom. Perturbations (c, d) of field and plasma in a shear Alfvén wave and in a fast compressional wave. The density of shading illustrates increases and decreases in the plasma density.

**FIG. 11.5.** Standing oscillations in a dipole field. Top: Schematic illustrations of the field displacements in a fundamental and second harmonic of the field-line resonances. Dashed lines are the displaced field lines. Bottom: Plots of the perturbation electric and magnetic fields versus distance along the field line from one ionosphere to the other.



where *n* is an integer. Recalling that for a shear Alfvén wave with  $k_{\parallel} = k_{\parallel} \cos \theta = 2\pi/\lambda_{\parallel}$  representing the component of **k** along the background field,

$$\omega = v_A k_{\parallel} = v_A 2\pi/\lambda_{\parallel}$$

it follows that the allowed frequencies of these waves standing on field lines are

$$f = nv_A/(2l) = nB/(2l\sqrt{\mu_0\rho})$$
 (11.21)

Thus, only certain resonant frequencies can be established. These frequencies are controlled by the length of the field lines between the ionospheres, the strength of the magnetic field, and the plasma density. If the field geometry is known, it is possible to infer the plasma density by measuring the frequencies of shear Alfvén waves present in a magnetic cavity bounded by the northern and southern ionospheres. This is just the point that Dungey (1954a,b) made in his early papers on waves in the magnetosphere. Figures 11.4c and 11.4d show how field and plasma might be deformed if standing Alfvén waves or compressional waves, respectively, perturbed the magnetosphere. For the former, the density remains constant. For the latter, the density changes as the fluxtube volume changes. The structures of the wave perturbations along the magnetic-field line are illustrated for the two lowest harmonics in Figure 11.5. The upper part of the diagram illustrates the displacement of the flux tube in a dipolar field for the fundamental (n=1) and second harmonic (n=2) of the standing waves. The lower diagrams show how the electric (E) and magnetic (b) perturbations vary with distance along the background field. Even and odd modes are identified by the symmetry of the transverse magnetic perturbations about the equator, where E=0,  $u_1=0$ , and field lines do not move.

## 11.7 MHD WAVES IN A DIPOLAR MAGNETIC FIELD

The foregoing discussion has concentrated on waves in a uniform background magnetic field. A model of the background magnetic field that is slightly more complicated, but considerably more realistic for a planetary magnetosphere, is a dipole field. For a cold plasma in a dipole field, the MHD waves are very similar to those discussed for a uniform plasma.

Consider first a perturbation that compresses the system at the last field line on the right in the model illustrated in Figure 11.4a. The motion may not be uniform along the field, and so the boundary field lines will bend and will move closer to the shell of field lines just inside the boundary, thereby increasing the magnetic pressure. The pressure perturbation propagates into the system, producing changes in the components of the field in the  $\hat{\nu}$  and  $\hat{s}$  directions (the coordinate system is shown in Figure 11.6). This type of perturbation can be identified as a fast-mode wave.

A perturbation that sets an entire shell of plasma into azimuthal motion creates a wave perturbation in the  $\hat{\varphi}$  direction (Figure 11.6) that bends the field without changing its magnitude. Such a wave is a shear Alfvén wave.

Under most circumstances, the two wave modes are coupled, meaning that it may not be possible to set up a compressional wave without setting up a shear Alfvén wave somewhere in the system. If the compressional wave is monochromatic (i.e., has a single frequency, say  $f_{\rm fast}$ ), the coupling will be strongest on a field line for which  $f_{\rm fast}$  is a resonant frequency, which means that it matches the frequency of a shear Alfvén wave that can stand on that field line. This is not unexpected, because any oscillating system responds strongly to a driving force that contains a signal at its natural or resonant frequencies. Both the Alfvén wave and the driving compressional wave have local maxima at the resonant field line.

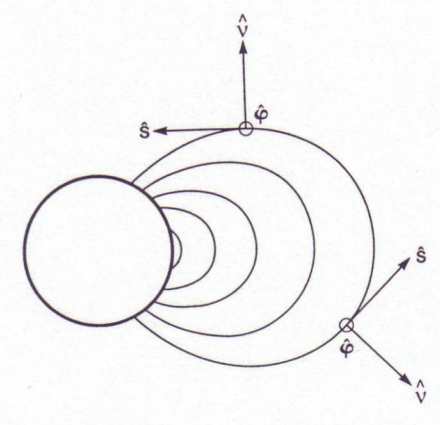


**FIG. 11.6.** Illustration of the unit vectors in a local dipole coordinate system at different latitudes.

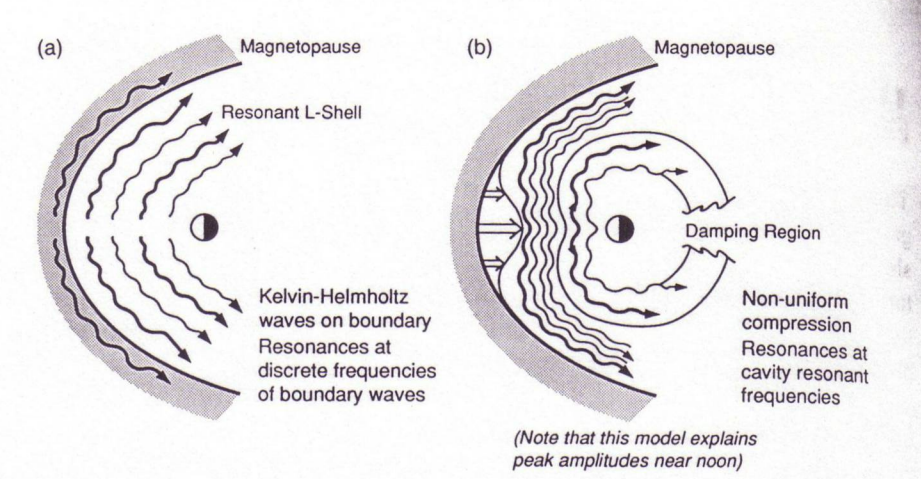
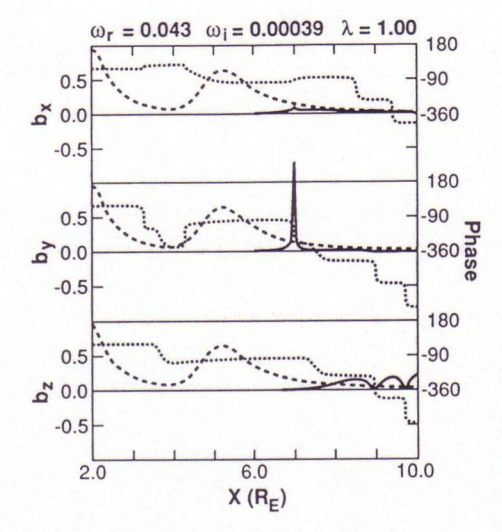


FIG. 11.7. Representations of wave perturbations throughout the dayside magnetosphere produced by (a) Kelvin-Helmholtz waves on the surface and (b) a compression of the nose of the magnetosphere.

Theories have been developed to describe how wave disturbances at the magnetopause boundary pump energy into the magnetospheric cavity and deposit it near magnetic shells where the conditions for the transverse resonances are satisfied (Southwood, 1974; Chen and Hasegawa, 1974; Kivelson and Southwood, 1986). A schematic illustration of this process, the field-line resonance theory of magnetospheric ULF waves, is shown in Figure 11.7a, where the waves are shown as wiggly lines moving away from local noon. The line thickness represents wave amplitude, which decreases inward but peaks locally at the resonant L shell. Eddy motions are induced within the magnetosphere by wave perturbations. The eddy flows reverse sense across amplitude extrema. Wave magnetic perturbations are proportional to flow perturbations, and this means that wave polarization also varies with location in the equatorial plane of the magnetosphere. As the wave must carry energy across the magnetic field, the wave mode coupling the boundary to the resonant field lines must be a compressional mode. The model assumes that the waves on the magnetopause are surface waves whose amplitude decays away from the surface. The polarization patterns shown can be mapped down to the ionosphere along magnetic-field lines. For Pc-5 waves (periods of 2.5-10 min), distributions of wave polarizations consistent with this model have been reported from ground observations (Samson and Rostoker, 1972). ULF waves have also been investigated by spacecraft using instrumentation to measure electric and magnetic fields and plasma flow velocities, and the theoretical picture of resonant field lines given here has received ample confirmation (Perraut et al., 1978; Takahashi and McPherron, 1982; Takahashi, McPherron, and Hughes, 1984).

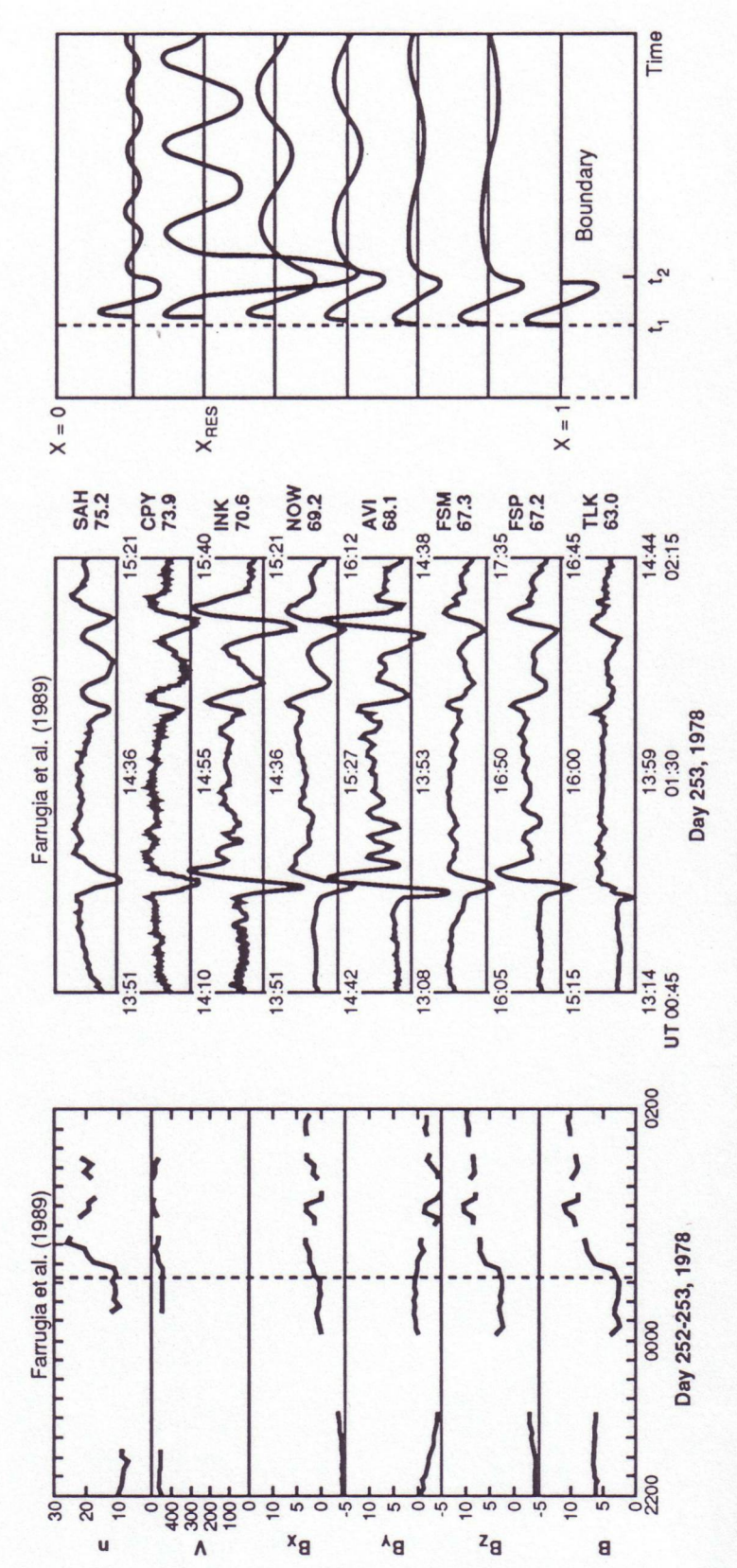
Recent work has focused on the response of the magnetosphere to impulsive perturbations on the boundary, such as those produced when the solar-wind dynamic pressure incident on the magnetopause changes abruptly. In connection with the response of the magnetosphere to an



impulsive source, the idea of the magnetosphere as a resonant cavity has recently been receiving renewed attention (Figure 11.7b). If the near-equatorial ionosphere and the magnetopause can serve to reflect signals propagating across the field, much as the northern- and southernhemisphere ionospheres serve to confine signals propagating along the field, the compressional wave frequencies will be quantized just as the shear Alfvén frequencies are quantized. Figure 11.8 shows characteristic wave amplitudes that would be established following an interval of transient impulsive disturbance in a box model of a magnetosphere with reflecting boundaries at the equatorial ionosphere and the magnetopause. The amplitude of the field-aligned component  $b_z$ , oscillates within an envelope of decreasing field strength. The  $b_v$  component (azimuthal in a realistic magnetosphere) is vanishingly small except in the immediate vicinity of the resonant field lines, at which the compressional and transverse frequencies match. The  $b_x$  component (radial in a realistic magnetosphere) shares qualitative features of the structures of  $b_{\nu}$  and  $b_z$ , with smaller amplitude.

The transient response that develops immediately following the impulsive disturbance of the boundary is itself of interest. Figure 11.9 shows an example of the types of signals that can be observed at the ground immediately following an impulsive disturbance in the solar wind. A sudden increase of solar-wind density, evident in the left-hand panels, sets up waves within the magnetosphere. A chain of ground stations recorded waves that were most intense and long-lasting near the middle of the chain. MHD wave theory for the magnetospheric cavity can provide an interpretation of these observations. The right-hand panel of Figure 11.9 shows schematically that cavity resonances produce waves of different characters on different field lines, with peak power and long duration at intermediate latitudes.

FIG. 11.8. The amplitude (solid traces) and phase (long dashes) of a global-mode wave versus equatorial distance in a box model of the magnetosphere with a spatially varying Alfvén speed (short dashes); z is field-aligned; x is the direction of the gradient of the Alfvén velocity. (From Zhu and Kivelson, 1989.)



ground magnetometers. Right: Predicted waves from a cavity model of the magnetosphere. time of the jump in dynamic pressure. Middle: Waves observed along a latitudinal chain of FIG. 11.9. An example of waves set up in the magnetosphere following an increase in solar-wind dynamic pressure. Left: Solar-wind data, with the dashed line indicating the (Data from Farrugia et al., 1989.)

### 11.8 SOURCES OF WAVE ENERGY

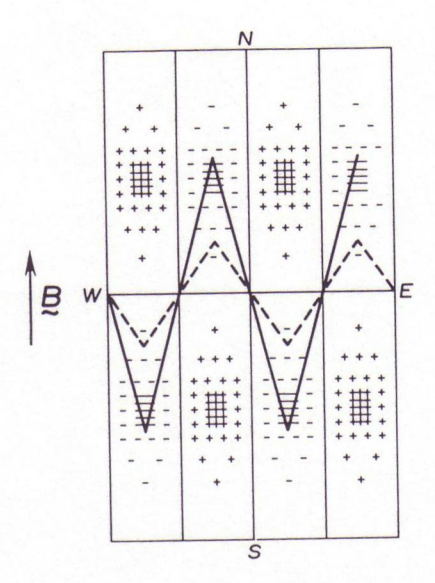
In describing the properties of ULF waves, we have not addressed the questions of wave generation. Diverse processes can excite waves, and several different driving mechanisms are important in generating the waves observed in the magnetosphere or the solar wind. Any process that modifies the equilibrium of the plasma and the field can serve as an energy source for waves. As for most magnetospheric phenomena, the energy comes principally from the solar wind, but other energy sources in the ionosphere or internal to the magnetosphere can be important.

The departure from equilibrium that drives the waves is often related to large-scale convective flows. In particular, the shear in the flow across the magnetopause can produce surface waves, of the sort mentioned in the preceding section, through what is called the Kelvin-Helmholtz instability. The process is closely related to the one that produces waves on the surface of a lake when a strong wind is blowing. These surface waves compress the magnetosphere, and the perturbations generate compressional waves that decay or propagate across field lines. Field-line resonances, described in the preceding section, couple the energy of compressional waves into shear Alfvén waves. Other compressional perturbations of the magnetopause can serve as sources of wave energy. Examples are the displacements of the magnetopause that occur when a solar-wind shock passes by, or those that are produced by time-varying dayside reconnection. Waves in the solar wind can be convected through the bow shock and under certain circumstances can introduce wave power into the magnetosphere.

Steady convective flows need not generate waves, but time-varying flows typically drive MHD waves. The time-varying convective flows can be generated within the magnetosphere (e.g., at the time of substorm onset), or they can be generated in the ionosphere (e.g., in regions locally heated by precipitation of energetic particles). In either case, when the motion of one end of a flux tube changes, waves grow and bounce back and forth along the flux tube until the entire flux tube begins to move as a whole.

Convection is not the only source of wave energy. Waves can grow when the velocity-space distribution of the plasma is not in an equilibrium configuration, either because it is anisotropic or because the particle energy distribution is anomalous. Unstable velocity-space distributions develop in the ring-current region when particles are injected by enhanced convection during substorms and storms. Then it is possible to find groups of particles that are in resonance with the waves; particles that can bounce and drift in phase with ULF waves, in some cases causing the wave power to grow. An example of particles in resonance with waves nominally in the Pc-3 to Pc-5 band is shown in Figure 11.10, which again uses the box model. Electric-field intensity is shown by the

FIG. 11.10. Schematic of two bouncing particles with different equatorial pitch angles and therefore different mirror fields drifting relative to a ULF wave that stands between the northern and southern ionospheres in a box model of the magnetosphere. The plus and minus signs represent the sign of a wave electric field, and their density indicates the amplitude of that field. The particle along the solid trajectory will experience greater acceleration or deceleration as it spends time in field regions of very strong perturbation.



density of symbols. The loci of the guiding centers of bouncing, drifting particles are shown as diagonal lines. The orbits have been chosen so that the particles drift through exactly one wavelength in each full bounce; they are resonant with the wave. The lines remain in regions of negative E and the ions on these paths will lose energy. Ions on the dashed-line orbit will gain energy, as they always experience E > 0. Nonresonant particles will move through both positive and negative E and therefore will not change energy, as viewed over multiple bounces.

The higher-frequency wave classes of Table 11.1 (Pc-1, some Pc-2 waves, and Pi-1) arise from a local interaction with ions in motion along the field. Particles can resonate with higher-frequency waves that, in the particle rest frame, match their gyrofrequency. This means that the particle gyrofrequency must equal the wave frequency Doppler-shifted to account for the velocity of the particle's motion along the field. Waves produced in this way are also found upstream of the bow shock, where ions that have been reflected back upstream from the bow shock produce ion-cyclotron instabilities in the solar wind. Resonances that fall into the Pc-1 and Pc-2 classes are ion-cyclotron resonances, which will be discussed in connection with other "kinetic" wave processes in Chapter 12.

### 11.9 INSTABILITIES

In Section 11.3, we linearized the equations that govern the plasma and fields, thereby obtaining wave solutions whose average amplitudes are constant in time. This implies that even over many wave cycles, the plasma neither loses energy to the waves nor gains energy from the waves. If, on the other hand, energy and momentum are transferred,

either from the waves to the plasma or from the plasma to the waves, the average wave amplitude will change with time.

Wave growth requires a source of free energy in the plasma. Plasma conditions that lead to nonlinear growth are referred to as instabilities. The plasma conditions that can lead to wave growth include beams. in which directed particle fluxes are superimposed on a plasma at rest, anisotropic distributions of particle pitch angles, and nonequilibrium spatial distributions of plasma. Thus, the departures from equilibrium that can lead to wave growth can be present either in the phase-space or in the configuration-space distribution.

If waves described by the time dependence of equation (11.12) are to grow,  $\omega$  must have a positive imaginary part (i.e.,  $\omega = \omega_0 + i\gamma$ , where both  $\omega_0$  and  $\gamma$  are real, and  $\gamma > 0$ ). Equation (11.12) shows that for positive  $\gamma$ , the amplitude grows exponentially with time. Therefore,  $\gamma$  is called the growth rate. Notice that if  $\gamma$  is negative, the wave decays.

An exponentially growing wave satisfies the linear approximation only for times short compared with  $1/\gamma$ ; at longer times, the waves become nonlinear, and the mathematical formulation that we have presented in this chapter is no longer applicable.

Some of the instabilities that can develop in a uniform background magnetic field are closely related to the linear waves introduced in this chapter. We shall identify only one example, the mirror instability. This instability of an anisotropic plasma requires that the perpendicular plasma pressure exceed the parallel pressure. The condition for wave growth of the mirror instability is

$$1 + \beta_{\parallel} (1 - \beta_{\parallel}/\beta_{\parallel}) < 0$$

where  $\beta_{\parallel}$  ( $\beta_{\parallel}$ ) is the ratio of  $p_{\parallel}$  ( $p_{\parallel}$ ) to the magnetic pressure. If this inequality is satisfied, the uniform field develops bubbles of low field strength separated by regions of enhanced field strength. Where the field is stronger than the unperturbed field, the particle mirror points shift in such a way that the plasma density decreases. Where the field is weaker than the unperturbed field, the plasma density increases. This field configuration reduces the anisotropy of the plasma and lowers the energy of the system.

The mirror instability is a purely growing wave with  $\omega_0 = 0$ . Notice that the phase relations between plasma and magnetic pressure are the same as in the slow mode, but this is a nonpropagating wave.

Wave instabilities make an important contribution to the configuration and transport properties of a magnetosphere. For example, changes in the curvature of the field can be produced by instabilities referred to as ballooning and firehose instabilities. Plasma stirring or even steady transport can, under appropriate circumstances, be produced by the interchange instability. In all cases, the perturbations grow because the plasma distribution is not in a minimum-energy state, and the nonlinear waves act to bring it closer to a minimum-energy configuration.

### 11.10 WAVES IN PLANETARY MAGNETOSPHERES AND ELSEWHERE

Although the discussion has focused on MHD waves present in the terrestrial magnetosphere, such waves are present wherever magnetized plasmas are subject to forces that introduce perturbations on appropriately long time scales (i.e., long with respect to the ion gyroperiod) Time-varying patterns of magnetic structure or of plasma flow are not normally imposed over the entire system simultaneously. Thus, nonequilibrium pressure gradients or flow patterns develop, and ULF waves can act to restore equilibrium. For example, if plasma is set into motion on one part of a magnetic-flux tube, the plasma elsewhere on the flux tube must respond to the changes. This requires signals to propagate along the flux tube. Signals that carry field-aligned current from one part of the flux tube (such as the equatorial magnetosphere or the solar corona) to another (say the ionosphere or the solar photosphere) are essential for getting the entire flux tube to move as an entity. Such signals must be carried by shear Alfvén waves.

MHD waves are observed in the solar wind; special forms of such waves are observed upstream of planetary bow shocks. The characteristic wave periods change linearly with the magnitude of the solar-wind magnetic field. The solar-wind flow convects these waves toward the magnetosphere, and they introduce wave power into the magnetospheric cavity. By monitoring the power in Pc-3 and Pc-4 waves (periods from tens of seconds to minutes) on the ground, the magnitude of the interplanetary magnetic field can be estimated.

The study of MHD waves in planetary magnetospheres is not yet complete, but one example will serve to illustrate the value of studying them. Figure 11.11 presents Voyager 2 data from Jupiter. Plotted are the perturbations of magnetic and particle pressures measured by the spacecraft instruments. The fluctuations are proportional to the fluctuations of the field-aligned component of the magnetic field. As the particle detector is not able to determine the mass of the ions that are detected, there is an uncertainty in the particle pressure. In this plot it has been assumed that the ions are protons. However, heavy ions like sulfur and oxygen are also known to be present in the Jovian magnetosphere. If the pressure were calculated assuming singly charged oxygen ions, the particle-pressure fluctuations would be larger by a factor of 10. Notice the anticorrelated changes between the two perturbation pressures. Recalling that the slow mode maintains the total pressure approximately constant and therefore corresponds to perturbations with anticorrelated particle and field pressures, it is natural to expect that these fluctuations represent a slow-mode type of disturbance. Yet, although these two fluctuating pressures are strongly anticorrelated, their sum is not constant. The amplitude of the particle-pressure fluctuations is about one-

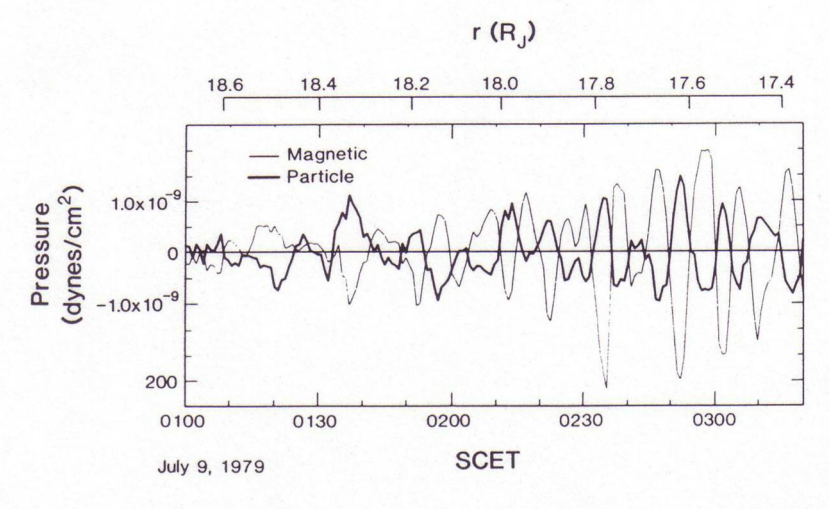


FIG. 11.11. Example of MHD waves observed in the Jovian magnetosphere by Khurana and Kivelson (1989). The particle and field pressures are in antiphase, as in slowmode or mirror-mode waves.

third that of the magnetic-pressure fluctuations. However, if the pressure were recalculated assuming that the plasma contains about 30 percent singly ionized oxygen ions, the total pressure fluctuations would become negligibly small. That possibly was the best available method for determining the composition of the intermediate-energy plasma population in the Jovian magnetosphere with measurements available from the *Voyager 1* and 2 spacecraft, but new data from the *Ulysses* flyby (February 1992) and ultimately from the *Galileo* spacecraft (1995) will provide direct composition measurements. Then we shall be able to evaluate the accuracy of our estimates based on an understanding of the properties of ULF waves.

#### ADDITIONAL READING

Below are listed some good review articles on ULF waves:

Southwood, D. J., and W. J. Hughes. 1983. Theory of hydromagnetic waves in the magnetosphere. *Space Sci. Rev.* 35:301.

Hughes, W. J. 1983. Hydromagnetic waves in the magnetosphere. In *Solar Terrestrial Physics*, ed. R. L. Carovillano and J. M. Forbes (p. 453). Dordrecht: Reidel.

Pilipenko, V. A. 1990. ULF waves on the ground and in space. J. Atmos. Terr. Phys. 52:1193.

Samson, J. C. 1991. Geomagnetic pulsations and plasma waves in the Earth's magnetosphere. In *Geomagnetism*, vol. 4 (p. 481). New York: Academic Press.

### **PROBLEMS**

- **11.1.** In regions of low plasma  $\beta$  in a dipole field, which represents much of the dayside magnetosphere, the cold-plasma approximation is appropriate.
  - (a) Use your knowledge of the properties of a dipole magnetic field  $(B_{eq} \propto L^{-3})$ , length of field line proportional to L, volume of flux tube

proportional to  $L^4$ , equation of field line  $r = LR_E \cos^2 \lambda$ ) to explain why the fundamental excitations of field lines at large L occur at lower frequencies than do the fundamental excitations of field lines at small L. Assume that the density is uniform (1 electron per 1 cm³) throughout the dipolar region of the magnetosphere and that at 6.6  $R_E$  the fundamental frequency is 14 mHz. Make a rough plot showing how the fundamental frequency varies with L.

- (b) Actually, the magnetospheric-plasma density often varies inversely with the flux-tube volume over large parts of the outer magnetosphere. Make a rough plot of the fundamental frequency of field-line excitations normalized to 14 mHz at  $6.6R_E$  in a dipole field assuming this type of variation for the density.
- (c) Although the density variation used in part (b) is a good approximation, the magnetospheric density actually drops by a factor of 100 or more across the plasmapause. Allow for a plasmapause at L=4, and assume that the density jumps by 100 inside the plasmapause. Again provide a rough plot of the fundamental frequency versus L.
- (d) Where on the surface of the earth would you expect to find pulsations of 50 mHz for the assumed conditions of part (c)?
- **11.2.** Suppose that a standing Alfvén wave is established on a field line at L=5, where the magnetosphere is approximately cylindrically symmetric. The ambient particle population is taken to include both energetic and cold plasma. Near the equator, the density is  $\rho$  in kilograms per cubic meter. Locally near the equator the uniform-field approximation is valid; the ambient field is  $B_0/L^3$  and is oriented along the z-direction. The standing wave is a superposition of waves with k parallel and antiparallel to  $\hat{\mathbf{z}}$ .
  - (a) Assume that the magnetic perturbation  $\mathbf{b}$  is radial. Determine the wave electric-field and the fluid-velocity perturbations as functions of  $\mathbf{b}$ ,  $\rho$ , and L. Pay attention to the vector character of the perturbations to determine their directions. Identify the direction of plasma displacement.
  - (b) The wave oscillations displace the plasma. The rate of displacement is slow enough that the plasma responds adiabatically. Show why this is true, using nominal dipole field values.
  - (c) Explain why you must consider the variations of particle flux with both L and W (particle energy) if you wish to determine how the particle flux measured at a spacecraft is modulated by a wave.
  - (d) Assume that only cold electrons and ions are present  $(W \approx 0)$ . Show that the magnitude of the density variations takes the form

$$\delta n = \frac{b(\partial n/\partial L)}{R_E \omega \sqrt{\mu_0 \rho}}$$

#### 11.3

(a) Plasma boundaries in the magnetosphere sometimes are described as standing fronts that can be thought of as waves propagating against a flow. Consider the high-latitude magnetopause in the noon-midnight meridian of the magnetotail for a strictly southward-oriented inter-

- planetary magnetic field. Sketch the change of the field across the boundary. Carefully consider the changes that must occur across the boundary. What MHD wave mode produces these changes?
- (b) Waves are detected in the solar wind as well as in the magnetosphere. Assume that the solar-wind magnetic field is oriented along the spiral angle. Wave perturbations with magnetic polarization perpendicular to the ecliptic plane are observed. What MHD wave mode is relevant to such perturbations?
- (c) Waves generated at the magnetopause can be observed behind the earth's bow shock. Only one of the MHD wave modes can travel from the magnetopause to the nose of the bow shock. Which wave mode is it, and how do you reach this conclusion?